Functional Consequences of RNA 5′-Terminal Deletions on Coxsackievirus B3 RNA Replication and Ribonucleoprotein Complex Formation

Nicolas Lévêque,[a,b]* Magali Garcia,[c] Alexis Bouin,[b] Joseph H. C. Nguyen,[b] Genevieve P. Tran,[b] Laurent Andreoletti,[a] Bert L. Semler[b]

EA-4684 CardioVir, Faculty of Medicine and University Hospital Center, University of Reims Champagne-Ardenne, Reims, France[a]; Center for Virus Research and Department of Microbiology and Molecular Genetics, School of Medicine, University of California, Irvine, California, USA[b]; EA-4331 LITEC, Faculty of Medicine and Pharmacy, University of Poitiers, Poitiers, France[c]

ABSTRACT Group B coxsackieviruses are responsible for chronic cardiac infections. However, the molecular mechanisms by which the virus can persist in the human heart long after the signs of acute myocarditis have abated are still not completely understood. Recently, coxsackievirus B3 strains with 5′-terminal deletions in genomic RNAs were isolated from a patient suffering from idiopathic dilated cardiomyopathy, suggesting that such mutant viruses may be the forms responsible for persistent infection. These deletions lacked portions of 5′ stem-loop I, which is an RNA secondary structure required for viral RNA replication. In this study, we assessed the consequences of the genomic deletions observed *in vivo* for coxsackievirus B3 biology. Using cell extracts from HeLa cells, as well as transfection of luciferase replicons in two types of cardiomyocytes, we demonstrated that coxsackievirus RNAs harboring 5′ deletions ranging from 7 to 49 nucleotides in length can be translated nearly as efficiently as those of wild-type virus. However, these 5′ deletions greatly reduced the synthesis of viral RNA *in vitro*, which was detected only for the 7- and 21-nucleotide deletions. Since 5′ stem-loop I RNA forms a ribonucleoprotein complex with cellular and viral proteins involved in viral RNA replication, we investigated the binding of the host cell protein PCBP2, as well as viral protein 3CD[pro], to deleted positive-strand RNAs corresponding to the 5′ end. We found that binding of these proteins was conserved but that ribonucleoprotein complex formation required higher PCBP2 and 3CD[pro] concentrations, depending on the size of the deletion. Overall, this study confirmed the characteristics of persistent CVB3 infection observed in heart tissues and provided a possible explanation for the low level of RNA replication observed for the 5′-deleted viral genomes—a less stable ribonucleoprotein complex formed with proteins involved in viral RNA replication.

IMPORTANCE Dilated cardiomyopathy is the most common indication for heart transplantation worldwide, and coxsackie B viruses are detected in about one-third of idiopathic dilated cardiomyopathies. Terminal deletions at the 5′ end of the viral genome involving an RNA secondary structure required for RNA replication have been recently reported as a possible mechanism of virus persistence in the human heart. These mutations are likely to disrupt the correct folding of an RNA secondary structure required for viral RNA replication. In this report, we demonstrate that transfected RNAs harboring 5′-terminal sequence deletions are able to direct the synthesis of viral proteins, but not genomic RNAs, in human and murine cardiomyocytes. Moreover, we show that the binding of cellular and viral replication factors to viral RNA is conserved despite genomic deletions but that the impaired RNA synthesis as-

sociated with terminally deleted viruses could be due to destabilization of the ribonucleoprotein complexes formed.

Coxsackie B viruses (CVBs), which belong to the genus *Enterovirus* of the family *Picornaviridae*, have nonenveloped icosahedral capsids composed of 60 copies each of the four structural proteins (VP1 to VP4) enclosing a single-stranded, positive-sense RNA genome of ~7,400 nucleotides (1). The genome consists of a single open reading frame encoding 11 mature proteins, flanked on both the 5′ and 3′ ends by noncoding regions (NCRs) (1–3). The enterovirus 5′ NCR is ~750 nucleotides in length and has several complex RNA secondary structures, including an internal ribosome entry site (IRES) involved in cap-independent translation and a 5′-terminal cloverleaf, or stem-loop I (S-L I), required for replication of the viral genome. Stem-loop I includes approximately the first 110 nucleotides of the 5′ NCR and is organized into one stem (a) and three stem-loop structures (b, c, and d), which bind cellular and viral proteins involved in viral RNA synthesis (4, 5). In the cytoplasm of infected cells, cellular poly(rC)-binding protein 2 (PCBP2) and the viral protein 3CD^{pro} bind stem-loops b and d of stem-loop I, respectively, at the 5′ end of the enterovirus genome. This ribonucleoprotein complex is required for the initiation of antigenomic (negative-strand) RNA synthesis, as well as genomic (positive-strand) RNA synthesis (4–10). PCBP2 also binds to a C-rich stretch of nucleotides located 3′ of stem a in S-L I (4, 11). In turn, heterogeneous nuclear ribonucleoprotein C (hnRNP C) is thought to bind to the cloverleaf at the 3′ end of antigenomic (negative-strand) viral RNA to facilitate the initiation of positive-strand RNA synthesis (12). These newly synthesized positive-strand RNAs are used either as mRNAs for further rounds of translation and RNA replication or as genomic RNAs packaged into virions for subsequent rounds of infection (3, 13).

The CVBs are common human pathogens, transmitted through fecal-oral and respiratory routes, and are considered the main viral cause of acute myocarditis in children and young adults in developed countries (14, 15). Following the acute phase, myocarditis can become chronic and progress toward the clinical stage of dilated cardiomyopathy (DCM). This disease state is characterized by right and left ventricle enlargement with systolic function impairment and chronic evolution toward complete heart failure, requiring heart transplantation. During the progression of disease from acute myocarditis to DCM, CVB can be detected in heart tissues and, more specifically, in cardiomyocytes. A correlation between enterovirus replication and poor clinical outcomes has been demonstrated, suggesting that persistent viral replication activities are potentially involved in disease progression (16–22). Moreover, expression of viral 2A proteinase alone in a murine model of CVB3 myocarditis has been shown to generate dilated cardiomyopathy (23). Expression of 2A can cause significant impairment of cardiomyocyte function through proteolytic cleavage of dystrophin, resulting in a decrease in cell contractility, an increase in membrane permeability, and a focal spread of the virus to adjacent cells (23–28). However, the molecular mechanisms by which the virus can persist in the heart from acute myocarditis to DCM are poorly understood, limiting the development of new specific therapeutic strategies.

Recently, Bouin and colleagues reported CVB3 strains harboring 5′-terminal genomic RNA deletions, ranging from 15 to 48 nucleotides in length, in explanted heart tissue collected from a 47-year-old immunocompetent woman suffering from idiopathic DCM (29). These terminal deletions, which partially removed 5′ S-L I sequences, mirrored results previously obtained by Chapman and colleagues, who demonstrated that terminal deletion (TD) mutations could occur in a patient naturally infected with CVB2 and suffering from fulminant myocarditis, in the heart and the pancreas in mice inoculated with wild-type (WT) CVB3, and during CVB3 passages in primary cell cultures

(30–32). However, these recent findings showed for the first time the existence of TD CVB genomic-RNA populations in a patient suffering from chronic cardiomyopathy.

Deletions involving sequences within the 5′ S-L I structure of genomic RNAs are known to cause profound changes in viral biology by reducing viral replication compared to wild-type viruses (3, 32–35). Indeed, the discovery of TD mutations in heart biopsy specimens was associated with low viral loads and abnormal positive-strand/negative-strand viral RNA ratios, close to 1 rather than the high ratios (30 to 70) normally observed in enterovirus-infected cells with wild-type viruses (32, 36–38). Moreover, TD variants of CVB3 replicate in both cell culture and tissues from experimentally inoculated mice and from naturally infected humans without apparent cytopathic effect (31, 32). Overall, 5′-terminal deletions within genomic RNAs could be a mechanism by which CVB can persist covertly in the heart long after the acute infection cycle with limited, but progressive, damage to the myocardium. A prolonged, persistent viral infection could then explain how chronic cardiomyopathies develop via the continuous synthesis of viral proteins with proapoptotic, immunomodulating, or other activities harmful to cardiac cell structures and functions.

To date, translation and RNA replication of 5′-terminally deleted CVB3 in a cardiac cell model have not been studied. Moreover, the mechanism by which deletions within the 5′ S-L I affect the replication of the viral RNA is still unknown. The aim of this study was to assess *in vitro* the consequences of the 5′ S-L I deletions observed *in vivo* for CVB3 replication. Using extracts of uninfected HeLa cells and cell culture transfection of luciferase replicons in two types of cardiomyocytes, we evaluated translation and RNA replication of full-length and 5′-terminally deleted CVB3 RNAs. These experiments demonstrated that CVB3 RNAs harboring 5′-terminal deletions of 7 to 49 nucleotides can be translated nearly as efficiently as those of wild-type strains. However, transfection of reporter RNAs harboring these deletions into cultured cardiomyocytes demonstrated a loss of detectable RNA amplification signal beyond the translation of input RNAs. *In vitro* replication experiments in HeLa cell extracts confirmed these findings, showing greatly reduced levels of negative- and positive-strand RNA synthesis in each of the terminally deleted RNAs. Among the terminally deleted CVB3 RNAs tested, RNA synthesis was observed only for those harboring deletions of either 7 or 21 nucleotides. The only RNAs produced from these deleted templates were double-stranded RNAs (dsRNAs) (without detectable single-stranded RNAs [ssRNAs]), suggesting an abnormal positive-strand/negative-strand RNA ratio near 1, similar to the ratios found *in vivo* for TD viruses (36).

Partial deletion of the 5′ S-L I sequences would be predicted to alter the binding sites of proteins involved in CVB RNA synthesis, possibly providing an explanation for the low levels of TD RNA replication. To address this possibility, we used RNA mobility shift assays to investigate the binding of the host protein PCBP2 and the viral protein 3CD^{pro} to the 5′ ends of deleted forms of positive-strand RNA. We found that binding of these cellular and viral replication factors was qualitatively conserved for the 5′-terminally deleted viruses, independent of the size of the deletion; however, the stability and/or protein binding affinity of the ribonucleoprotein complexes decreased with the increase in size of the deletion, since they required higher protein concentrations to form. Overall, this study provides an *in vitro* analysis of RNP complexes that may be involved in persistent forms of CVB3 observed *in vivo* from heart tissues. Our data suggest a possible explanation for the low levels of RNA replication of deleted strains as a result of the consequences of the deletions for the formation of the RNP complex. In addition, these data raise the question of the capacity of some of the deleted strains to replicate autonomously, since no significant levels of RNA synthesis were detected for 5′-terminal deletions larger than 21 nucleotides.

RESULTS

Terminally deleted CVB3 RNAs are defective in replicon reporter assays. Deletions of CVB3 strains detected in patients suffering from DCM involved the 5′ terminus of the viral genome, which is a noncoding region but crucial for the regulation of
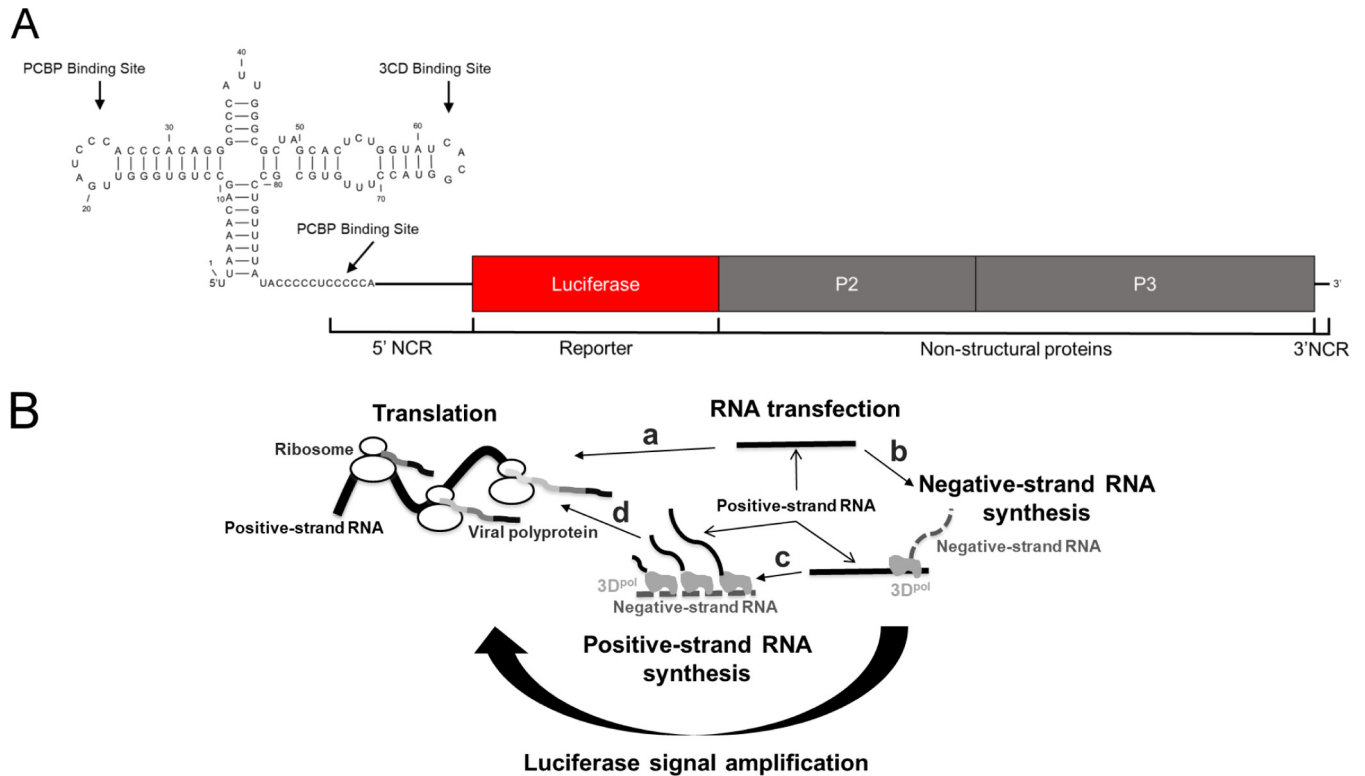
FIG 1 Schematic representation of luciferase replicon and signal amplification mechanisms through transfected replicon replication. (A) Schematic representation of the replicon. The replicons consisted of the CVB3-28 genome (74), in which the region encoding the capsid proteins (P1) has been replaced with a *Renilla* luciferase reporter gene. Deletions from 7 to 49 nucleotides in length were inserted at the 5′ end of the viral genome. The CVB3-0 replicon was generated from the CVB3-28 replicon by site-directed mutagenesis of nucleotide 234 (T in 28 and C in 0). (B) Replicons are positive-strand RNAs in which the P1 (capsid-coding) region has been replaced with a *Renilla* luciferase-coding gene. Following transfection, replicons are directly translated into viral polyprotein, including *Renilla* luciferase (a), or, following initial rounds of translation, used as a template for negative-strand RNA synthesis (b). Negative-strand RNAs in turn serve as templates for synthesis of positive-strand RNA (c), whose translation (d) leads to luciferase signal amplification.

translation and virus replication mechanisms. To determine the effects of these deletions on virus replication, we transfected full-length or deleted luciferase replicons, with 7- to 49-nucleotide deletions at the 5′ end of the viral genome, into heart-derived cells relevant for the pathophysiology of DCM: primary human cardiomyocytes (HCM) and a murine cardiomyocyte cell line (HL-1) (Fig. 1A). As shown in Fig. 1B, the replicon reporter produces a luciferase signal that is highly amplified if the input templates are translated and replicated. Luciferase activity was measured at 2 h posttransfection, a time at which transfected replicon RNA is being translated prior to replicon replication. This signal was similar for all of the replicons, independent of the size of the deletion or the type of cardiac cells (Fig. 2). However, if the incubation was extended beyond 2 h, a significant difference in luciferase activity was observed starting at 2 h posttransfection for both wild-type strains (CVB3-28 and CVB3-0), increasing by up to 2 log$_{10}$ units above the luciferase levels produced by the replicons harboring terminal deletions (Fig. 2). This difference was likely due to a lack of replication from the deleted genomic RNAs, causing reduced numbers of nascent genomic RNAs, resulting in reduced luciferase signal amplification (Fig. 1).

To test whether the reduced level of luciferase signals in cells transfected with replicons harboring 5′-terminal deletions was due to RNA synthesis defects, we carried out luciferase assays following transfection of replicons into cardiomyocytes with guanidine hydrochloride (GuHCl) in the cell culture medium. GuHCl is a potent inhibitor of enterovirus RNA replication targeting the 2C protein (39). In the absence of GuHCl, the increase in the luciferase signal over time following replicon transfection is the sum of both virus translation and RNA replication through translation of newly synthesized positive-strand RNAs, leading to luciferase signal amplification (the scheme is depicted
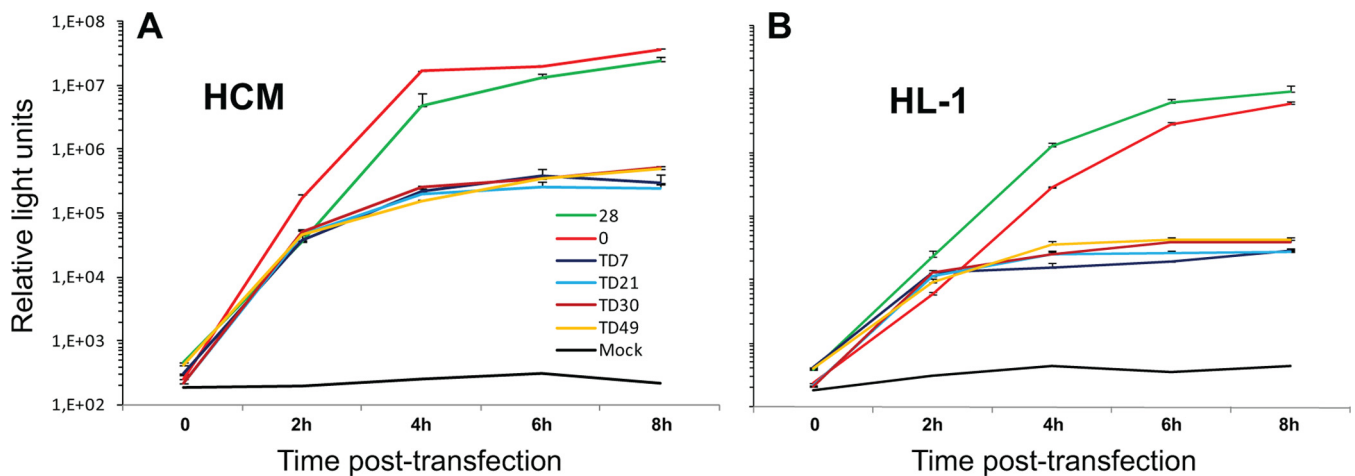
FIG 2 CVB3 replicon assays in two types of cardiomyocytes using wild-type (full-length) and TD replicon RNAs. Luciferase replicons were transfected into primary HCM (A) or in a continuous line of murine cardiomyocytes from an atrial tumor (HL-1 cells) (B). Luciferase activity was measured from 2 to 8 h posttransfection. The data presented are the results of three independent experiments. The error bars indicate standard deviations.

in Fig. 1). In the presence of GuHCl, the luciferase signal represents only translation from the input replicon RNA. Thus, the difference between luciferase signals measured in the absence and presence of GuHCl provides an assessment of virus genomic-RNA replication. The two cardiac myocyte types were transfected with deleted and wild-type replicons in the presence or absence of GuHCl. A 2-log-unit reduction of luciferase activity was observed after GuHCl treatment of human and murine cardiomyocytes transfected with the replicons generated from wild-type strains 28 and 0 (WT-28 and WT-0)) (Fig. 3A and B). However, no decrease in the luciferase signal was observed in GuHCl-treated cells transfected with the deleted replicons in comparison to the untreated cardiac cells (Fig. 3C and D). The limited effect of GuHCl on the luciferase signal produced by the terminally deleted replicons suggests that the signal was the result of input replicon translation without RNA replication.

Translation of TD genomic RNAs compared to wild-type CVB3 RNA. Although the observed deletions affected only the cloverleaf or S-L I in the 5′ NCR, a secondary-structure element required for RNA replication, and did not involve the IRES that is required for protein synthesis, the deletions may nevertheless have consequences for the stability or overall structure of viral RNA and thus affect translation. In addition, the pathophysiology of DCM in humans is partially explained by expression of the viral 2A proteinase, which cleaves dystrophin, a cardiac myocyte cytoskeletal protein. Therefore, it was important to determine the translation patterns and efficiencies directed by TD RNAs found during persistent CVB3 infections in the myocardium. Using *in vitro*-transcribed RNAs synthesized from six plasmid constructs containing the cDNAs of two wild-type strains (cardiovirulent [CVB3-28] and noncardiovirulent [CVB3-0] in mice) and of four TD strains with deletions ranging from 7 (TD7) to 49 (TD49) nucleotides, we carried out *in vitro* translation assays in a cytoplasmic extract (S-10) from uninfected HeLa cells in the presence of [^{35}S]methionine. Viral translation products were resolved by SDS-polyacrylamide gel electrophoresis and visualized by fluorography. To determine the relative levels of viral proteins synthesized by each RNA, signals detected on the gel for viral proteins 3CD, P2, VP1, VP3, 2A, and 2AB (collectively) were quantified. WT-0 0.4-μg RNA template (Fig. 4, lane 2) was set as the 100% reference control. Transcripts produced from the WT-0 construct do not have a hammerhead ribozyme at their 5′ termini, while the transcripts from the WT-28, TD7, TD21, TD30, and TD49 constructs contain a hammerhead ribozyme at their 5′ termini to generate authentic 5′-terminal CVB3 sequences. The additional, nonviral sequences present at the 5′ termini of WT-0 transcripts may account for the slightly reduced differences in translation efficiency compared to WT-28 and some of the TD transcripts. Overall, the data displayed in Fig. 4 show similar patterns of translation products for all RNAs tested,
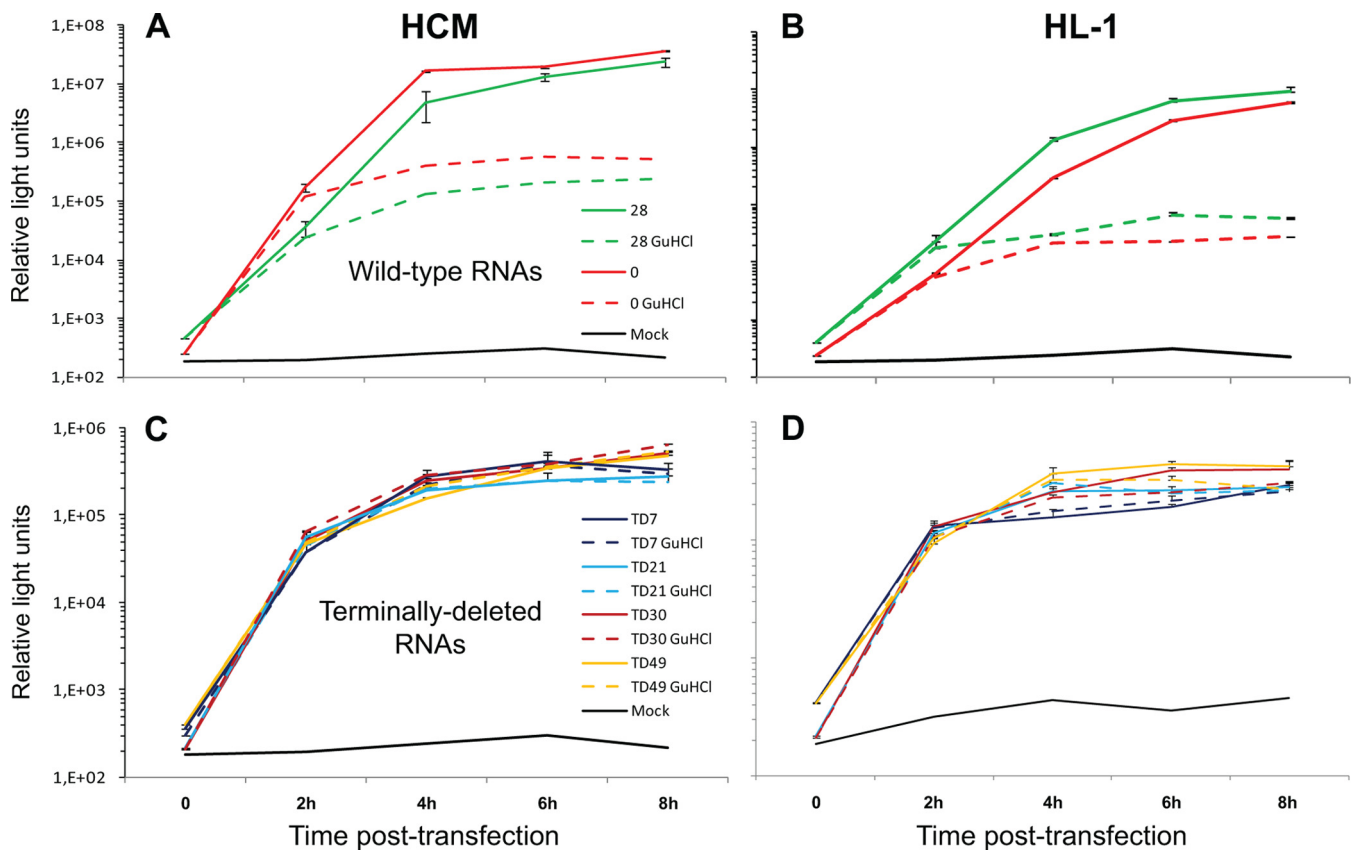
FIG 3 Impact of GuHCl treatment on full-length and terminally deleted luciferase replicon kinetics. Full-length (A and B) and deleted (C and D) luciferase replicon transcripts described in the legend to Fig. 2 were transfected into human (HCM) (A and C) and murine (HL-1) (B and D) cardiac myocyte monolayers in the presence or absence of GuHCl (an inhibitor of enterovirus RNA replication) at a final concentration of 3 mM. At 2, 4, 6, and 8 h posttransfection, cells were harvested and luciferase activity was measured. The y axis shows $\log_{10}$ units of luciferase activity. Luciferase units in the presence and absence of GuHCl are shown in each graph. Although not readily visible, standard deviations (as error bars) are given for each data point. The results presented are the products of three independent experiments.

although the RNAs with the largest deletions (TD30 and TD49) produced lower overall levels of CVB3 proteins, particularly at the lower concentrations of RNA. Transcripts corresponding to the TD30 deletion of CVB3 RNA reproducibly produced lower levels of viral proteins following *in vitro* translation (Fig. 4, lanes 10 and 11), even at much higher RNA concentrations (unpublished observations), suggesting that this deletion may have affected the overall structure of the 5′ NCR, including the IRES element.

***In vitro* RNA synthesis directed by TD RNAs is impaired.** Given that RNA amplification of the luciferase signal following transfection of cultured cells requires the synthesis of new positive-strand RNAs, it is possible that the TD RNAs may still be capable of negative-strand RNA synthesis, but not positive-strand RNA synthesis. To test this possibility, we performed an *in vitro* RNA replication assay by adding [³²P]CTP to *in vitro* translation assays that had progressed for 4.5 h and incubating the assay mixtures for an additional 2 h at 34°C. Newly synthesized RNAs were then visualized following electrophoresis on an agarose gel (Fig. 5). Replication of RNA corresponding to wild-type strains CVB3-28 and CVB3-0 was readily detected (Fig. 5). Both ssRNA (positive strand) and dsRNA (replicative intermediate [RI] or replicative form [RF]) were detected during replication of CVB3-28 RNA, whereas only dsRNAs were observed for CVB3-0. The plasmid DNA template encoding CVB3-28 RNA harbors a hammerhead ribozyme at the 5′ end of the transcript (32), which produces an authentic CVB3 5′ terminus. This transcript is an efficient template for negative-strand RNA synthesis and subsequent rounds of positive-strand RNA synthesis. In contrast, *in vitro* RNAs produced from pCVB3-0 have no hammerhead ribozyme at the 5′ end and harbor nonviral sequences that result in inefficient ssRNA (positive-strand) synthesis (13, 35). As noted
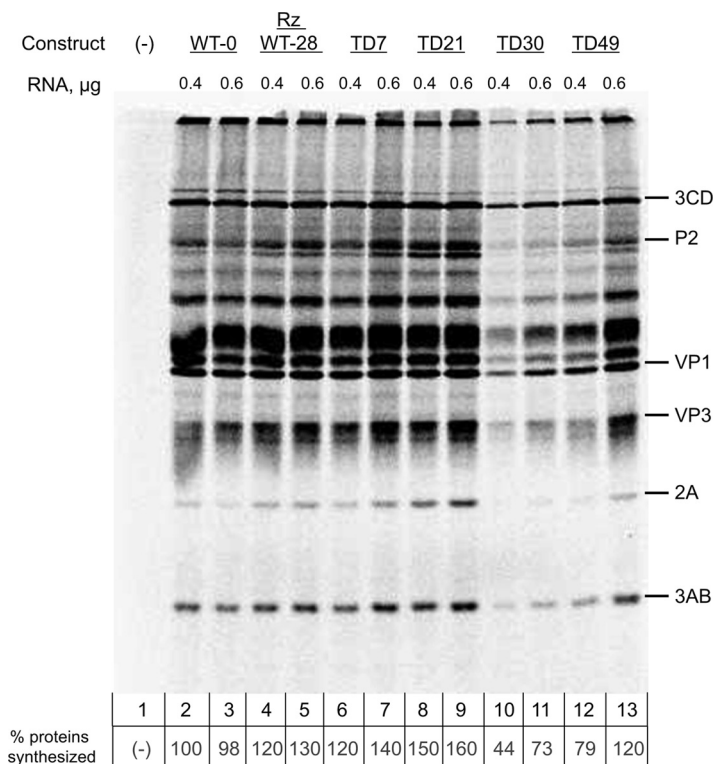
FIG 4 *In vitro* translation assay of wild-type and TD coxsackievirus B3 RNAs. Either 0.4 μg or 0.6 μg of viral RNA transcript was incubated for 6 h at 30°C in HeLa S10 cytoplasmic extract in the presence of [^{35}S]methionine. Labeled viral proteins (indicated on the right of the gel) were analyzed by SDS-PAGE and visualized by fluorography. Shown are representative data from four independent experiments. The first lane (−) is a translation reaction mixture incubated in the absence of transcript RNA. To determine the relative levels of viral proteins synthesized by each RNA, signals detected on the gel for viral proteins 3CD, P2, VP1, VP3, 2A, and 2AB (collectively) were quantified using ImageJ software (https://imagej.net/ImageJ). The second lane (WT-0 0.4 μg RNA template) was set as the 100% reference control. Transcripts produced from the WT-0 construct do not have a hammerhead ribozyme at their 5′ termini, while the transcripts from the WT-28, TD7, TD21, TD30, and TD49 constructs all contain a hammerhead ribozyme at their 5′ termini.

above, all TD transcripts harbor a hammerhead ribozyme at their 5′ termini, producing authentic 5′-terminal CVB3 sequences. Among the CVB3 TD RNAs, RNA synthesis was observed only for template RNAs harboring 7- or 21-nucleotide deletions, which were the smallest deletion sizes tested (Fig. 5). No RNA replication was detected for deletions of 30 or 49 nucleotides (Fig. 5, lanes 10 through 13). Moreover, RNAs detected during TD7 and TD21 replication were dsRNAs (i.e., RF and RI) resulting from negative-strand RNA synthesis with only very low levels of ssRNA (positive strand), as shown in Fig. 5, lanes 6 through 9, even though all of the TD RNA transcripts harbored a self-cleaving ribozyme at their 5′ ends. Overall, the results from our *in vitro* RNA replication assays, as well as from transfections of luciferase replicons into cardiomyocytes (with or without GuHCl), suggest that only TD7 and TD21 are capable of RNA replication, although positive-strand RNA synthesis was greatly reduced compared to wild-type RNAs.

Binding of cellular and viral proteins to RNAs harboring deletions of sequences within stem-loop I of the CVB3 5′ NCR. The drastic reduction of TD RNA synthesis capabilities could be explained by the removal of binding sites on the viral RNA for viral and cellular proteins involved in ribonucleoprotein complex formation required for RNA replication. The cloverleaf, or S-L I, at the 5′ end of positive-strand enterovirus RNAs is the binding site for the cellular protein PCBP2 and the viral protein 3CD^{pro}. The binding of these two proteins forms a ribonucleoprotein complex required for the initiation of negative-strand, as well as positive-strand, RNA synthesis (5, 7, 10, 40), as depicted in
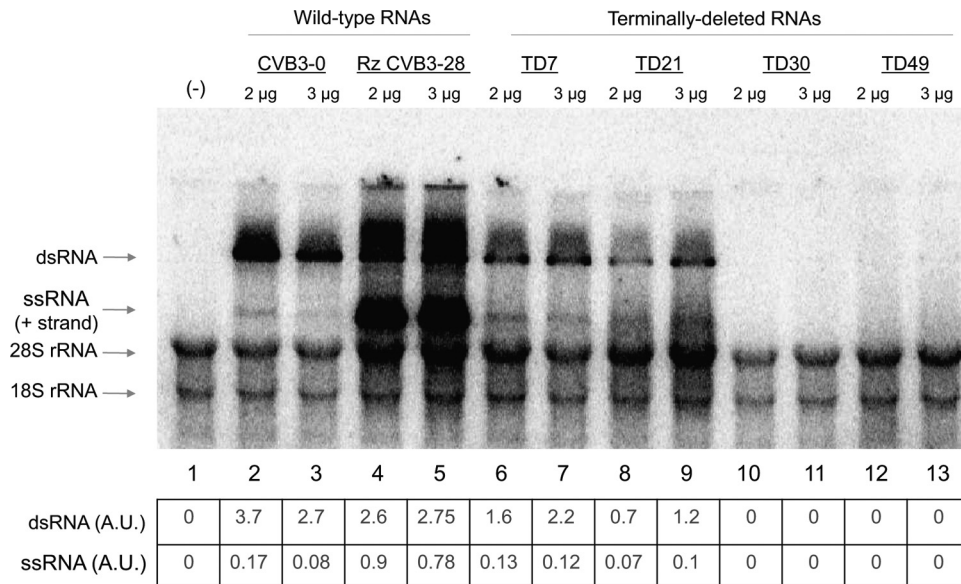
FIG 5 *In vitro* RNA replication of wild-type and TD coxsackievirus B3 transcripts. After a 4.5-h *in vitro* translation assay allowing the synthesis of nonstructural proteins in the absence of [^{35}S]methionine, the reaction mixture, consisting of viral transcripts (2 μg or 3 μg) and HeLa S10 cytoplasmic extract, was incubated for an additional 2 h at 34°C for RNA synthesis in the presence of [α-^{32}P]CTP. The purified RNA was then resolved on a 1.1% agarose gel in Tris-borate-EDTA buffer containing ethidium bromide. The amounts of 18S and 28S rRNA in each lane were used to confirm equal loading of samples in the gel. Plasmid DNA template encoding CVB3-28 RNA harbors a hammerhead ribozyme at the 5′ end of the transcript (32), producing an authentic CVB3 5′ terminus. This RNA is an efficient template for negative-strand RNA synthesis and subsequent rounds of positive-strand RNA synthesis. *In vitro* RNAs produced from pCVB3-0 have no hammerhead ribozyme at the 5′ end and harbor nonviral sequences that result in efficient negative-strand RNA synthesis but very inefficient positive-strand RNA (ssRNA) synthesis (13, 35). All TD transcripts harbor a hammerhead ribozyme at their 5′ termini, producing authentic 5′-terminal CVB3 sequences. The signals detected in the gel for single-stranded and double-stranded viral RNAs were quantified using ImageJ software. The signals were normalized to the 28S and 18S rRNA levels (collectively) for each sample and expressed in arbitrary units (A.U.). Lane 1 (−) shows the results of incubation of the *in vitro* replication reaction mixture in the absence of transcript RNA.

Fig. 6. We therefore investigated the interactions between the deleted positive-strand RNAs and the two proteins involved in viral RNA replication complex formation. The binding of deleted positive-strand viral RNA to PCBP2 and 3CD^{pro}, either alone or in combination, was analyzed by RNA mobility shift assays performed using recombinant proteins and RNA probes containing 5′ S-L I, including the adjacent C-rich sequences, generated by transcription of linearized, deleted cDNA CVB3 constructs. RNA corresponding to S-L I-containing sequences from the wild-type CVB3 28 strain was used as a positive control. Radiolabeled CVB3 S-L I-containing RNA was incubated alone or with

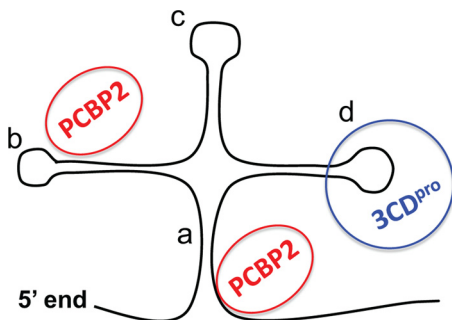**FIG 6** Schematic representation of cellular and viral proteins binding to the cloverleaf (stem-loop I) of positive-strand viral RNAs. Stem-loop I RNA is organized into stem a and stem-loops b, c, and d. Cellular PCBP2 and the viral protein 3CD^{pro} bind to the cloverleaf at the 5′ end of positive-strand RNA to form a ribonucleoprotein complex required for the initiation of both negative-strand and positive-strand RNA synthesis.
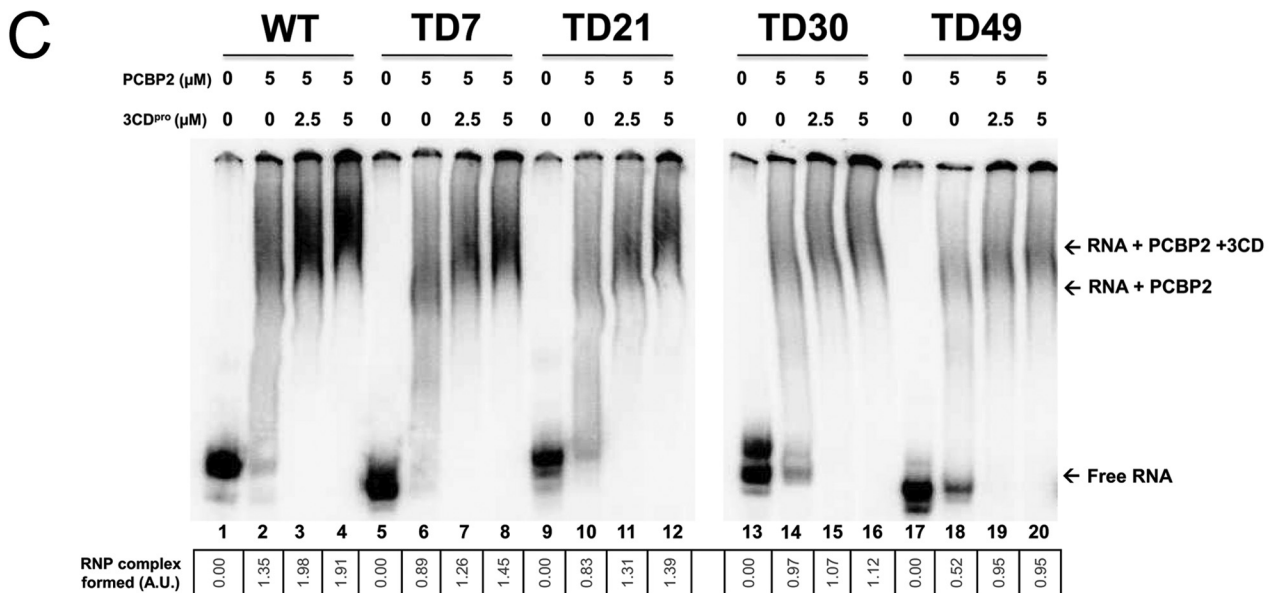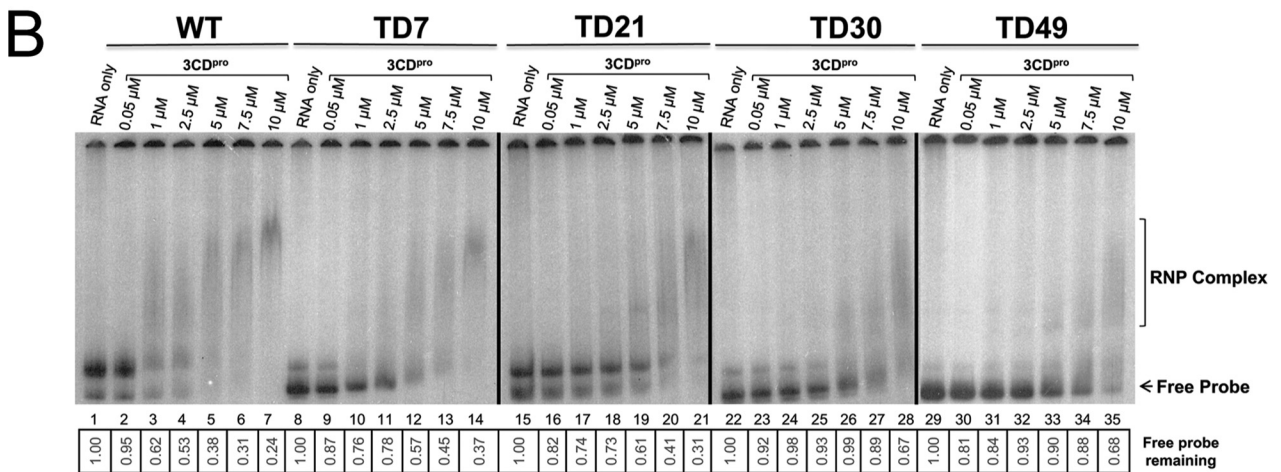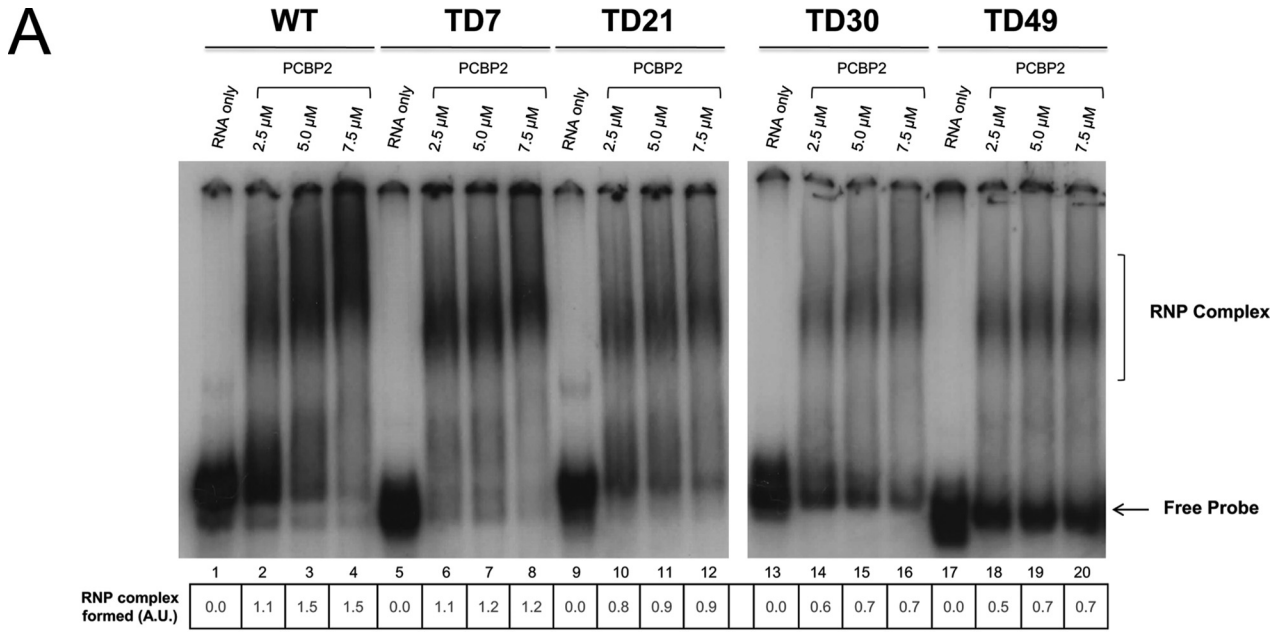
increasing concentrations of recombinant purified PCBP2 ranging from 2.5 μM to 7.5 μM. Resolution following electrophoresis on a native polyacrylamide gel showed RNP complex formation through a slower migration of all the RNA probes incubated with PCBP2, demonstrating protein binding even with the deletion of 49 nucleotides disrupting stem-loop b of S-L I, previously described as a PCBP2 binding site (Fig. 7A). However, the data displayed in Fig. 7A, lanes 9 through 20, demonstrate that the efficiency of complex formation is reduced when templates of deletions of increasing size (21, 30, or 49 nucleotides) are incubated with equivalent concentrations of PCBP2, as shown by decreased levels of RNP complexes and increased levels of free probe RNAs. Using imaging software to quantify band densities of RNP complexes formed under these experimental conditions, we estimate that TD7 transcripts bind PCBP2 at levels approximately 80% of those of WT RNA, while TD21 transcripts bind at approximately 60% compared to WT RNA. For the TD30 and TD49 transcripts, binding efficiency was less than half of that of WT RNA at the highest concentrations of PCBP2 used in our mobility shift assays.

When deleted forms of CVB3 S-L I-containing RNAs were incubated with recombinant purified 3CD^{pro} at concentrations ranging from 0.05 μM to 10 μM, all of the TD positive-strand RNAs were capable of binding 3CD^{pro}, as shown in Fig. 7B. As we observed for PCBP2 binding to these same deleted forms of RNA, RNP complex formation was associated with the disappearance of the free probe on the gel and a dose-dependent increase in the formation of slower-migrating species, with constructs harboring larger deletions requiring increased concentrations of 3CD^{pro} to form slower-migrating complexes. A 1 μM concentration of 3CD^{pro} was necessary for RNP complex formation with wild-type CVB3-28 S-L I-containing RNA, whereas 7.5 μM and 10 μM 3CD^{pro} were required for complete complex formation for TD21 and TD49 RNAs, respectively. As with the experiments describing RNP complex formation with recombinant PCBP2, we used imaging software to quantify band densities of RNP complexes formed between WT and TD RNAs and recombinant 3CD. Because the RNP complexes formed with 3CD are diffuse and difficult to quantify directly, we used the disappearance of radiolabeled probe as a measure of RNA-protein complex formation. As shown at the bottom of Fig. 7B, TD7 and TD21 transcripts formed RNP complexes with 3CD at efficiencies approximately 80 to 90% of that of WT RNA. In contrast, RNAs corresponding to TD30 and TD49 were able to form complexes with recombinant 3CD at levels less than 50% of that of WT RNAs.

To analyze ternary-complex formation, increasing amounts of 3CD^{pro} ranging from 0 to 5 μM were added to RNA binding reaction mixtures containing a fixed concentration of PCBP2 (5 μM) and a constant amount of labeled S-L I-containing probe. The results from these electrophoretic mobility shift experiments showed a supershifted RNP complex generated from deleted viruses when incubated with the two proteins simultaneously, confirming that deleted forms of CVB3 S-L I were capable of binding these two replication factors (Fig. 7C). Consistent with the data shown in Fig. 7A and B, the efficiency of this binding (and ternary-complex formation) decreased with the increasing size of the deletion, as demonstrated by the reduced levels of RNP complex formation (Fig. 7C, lanes 5 through 20). At the highest concentrations of PCBP2 and 3CD used in our assays, quantitation of the band densities of RNP complexes in Fig. 7C revealed that TD7 and TD21 RNAs bound proteins at levels between 70 and 80% of those of WT RNAs, while TD30 and TD49 were capable of complex formation at only 50 to 60% efficiency compared to WT CVB3 RNA.

DISCUSSION

Enteroviruses are primarily known for their involvement in acute infections, such as aseptic meningitis; upper or lower respiratory tract infections; hand, foot, and mouth disease; or acute myocarditis (41). Nonetheless, the role of enteroviruses as the etiologic agents of chronic diseases in the context of persistent viral infection has been described with increasing frequency. Several studies have associated persistent enterovirus infection with chronic diseases, such as amyotrophic lateral sclerosis, postpolio syn-

drome, chronic fatigue syndrome, type 1 diabetes, and chronic cardiomyopathy (i.e., chronic myocarditis and dilated cardiomyopathy) (16–20, 42–47). These chronic cardiac infections involved group B coxsackieviruses. However, the mechanisms leading to CVB persistence in the heart, as well as the link between viral persistence and the development of chronic cardiomyopathy, are not well understood. In 2005, Kim and colleagues identified variants of CVB in hearts of mice inoculated with wild-type CVB3 that contained terminal deletions in the 5′ NCRs of their genomic RNAs (32). These studies provided a possible link between the generation of noncytopathic viruses via genomic-RNA terminal deletions and the establishment and/or maintenance of persistent infections. Recently, similar deletions have been detected for the first time in cardiac biopsy specimens from patients suffering from chronic cardiomyopathy (29, 36). These deletions, ranging from 15 to 48 nucleotides in length, involved a 5′ RNA secondary structure (S-L I) that is the binding site for both viral and host cell proteins forming RNA replication complexes. Subsequently, Smithee and coworkers reported that CVB TD populations displayed impaired replication, with RNA levels 100,000-fold lower than those of wild-type virus (48). With the exception of the largest identified deletion of 49 nucleotides, the specific impacts of the different sizes of genomic deletions detected during persistent cardiac infections in mice or humans on the translation and replication of viral RNA had not been analyzed prior to the present study. Moreover, previous studies on TD virus replication have been mainly performed in noncardiac cell lines or cell-free reactions, with very little data about TD replication in cardiomyocytes, the cell type infected *in vivo*. Finally, the suggestion that altered formation or stability of replication complexes with deleted forms of viral RNA might be the explanation for impaired replication of TD viruses has so far not been investigated.

The work described in this study is the first use of cardiac myocyte cultures to assess the consequences of enterovirus genomic RNA deletions, detected in patients with chronic cardiomyopathy, on CVB3 translation and RNA replication. Transfection of deleted and nondeleted luciferase replicons in two types of heart cells demonstrated that at 2 h posttransfection, equivalent levels of luciferase activity were detected, corresponding to the translation of input RNA prior to the onset of genome amplification by RNA replication. These results were confirmed by *in vitro* translation reactions in HeLa cell S10 extracts, which showed nearly equivalent levels of protein synthesis among deleted and wild-type CVB3 RNAs. Taken together, our cell culture reporter transfection experiments and *in vitro* assays demonstrated the ability of TD RNAs harboring deletions of up to 49 nucleotides to synthesize viral proteins.

CVB protein expression could, in part, be involved in DCM pathophysiology due to the expression of the viral 2A proteinase in infected cardiomyocytes (23). In cardiomyocytes, this viral protein has been shown to cleave the host cell protein dystrophin,

FIG 7 Electrophoretic mobility shift assays with CVB3 5′ probes. Radiolabeled transcripts that included stem-loop I (approximately 175 to 225 nucleotides in length) corresponding to the 5′ end of coxsackievirus B3 positive-strand RNA were used in electrophoretic mobility shift assays to determine the ability of the 5′-terminally deleted RNAs (TD7, TD21, TD30, and TD49) to form RNP complexes with PCBP2 and 3CD^{pro}, alone or in combination. Full-length (wild-type) S-L I-containing RNA from CVB3 28 was used as a positive control. (A) [^{32}P]UTP-radiolabeled CVB3 S-L I-containing RNA was incubated alone (lanes 1, 5, 10, 13, and 17) or with increasing concentrations of recombinant purified PCBP2 ranging from 2.5 μM (lanes 2, 6, 10, 14, and 18) to 5 μM (lanes 3, 7, 11, 15, and 19) and 7.5 μM (lanes 4, 8, 12, 16, and 20). Note that samples from WT, TD7, and TD21 RNP complexes were analyzed on a gel separate from the one used to analyze TD30 and TD49, indicated by the white space between the two sets of lanes. (B) [^{32}P]UTP-radiolabeled CVB3 S-L I-containing RNA was incubated without (lanes 1, 8, 15, 22, and 29) or with increasing concentrations of a proteolytically active form of recombinant purified CVB3 3CD^{pro} that is incapable of self-cleavage at the 3C-3D junction (3CD[μ10]) ranging from 0.05 μM (lanes 2, 9, 16, 23, and 30) to 1 μM (lanes 3, 10, 17, 24, and 31), 2.5 μM (lanes 4, 11, 18, 25, and 32), 5 μM (lanes 5, 12, 19, 26, and 33), 7.5 μM (lanes 6, 13, 20, 27, and 34), and 10 μM (lanes 6, 14, 21, 28, and 35). Note that samples from WT and TD7 RNP complexes, TD21 RNP complexes, TD30 RNP complexes, and TD49 RNP complexes were analyzed on separate gels, indicated by the black vertical lines between the four sets of lanes. (C) To analyze supershifted ternary-complex formation, increasing amounts of 3CD^{pro} ranging from 0 (lanes 2, 6, 10, 14, and 18) to 2.5 μM (lanes 3, 7, 11, 15, and 19) and 5 μM (lanes 4, 8, 12, 16, and 20) were added to a fixed concentration of PCBP2 (5 μM). Lanes 1, 5, 9, 13, and 17 contained S-L I-containing probes alone. Note that samples from WT, TD7, and TD21 RNP complexes were analyzed on a gel separate from the one used to analyze TD30 and TD49, indicated by the white space between the two sets of lanes. Following incubation, RNP complexes were resolved on a native 4% polyacrylamide gel. The arrows and brackets on the right of the gels indicate probe alone (free probe), RNP complex formation, and ternary complex formation. The results shown are representative of three independent sets of experiments. The signals detected on polyacrylamide gels for RNP complex formation were quantified using ImageJ software. (A and C) The values were calculated by dividing the value of the complex signal by the value of free probes in the "RNA only" lanes incubated without proteins. Final amounts were obtained by subtracting the RNA only values from the calculated amounts. (B) The values represent the signal of free probe subtracted from the value of free probe in the RNA only lane (arbitrarily set at 1).

which links actin filaments to the plasma membrane (26, 27). Cleavage occurs in the hinge 3 region of dystrophin and is sufficient to induce cardiomyopathy with disruption of the sarcolemmal membrane and loss of normal localization of dystrophin in the heart (27). Dystrophin cleavage also promotes viral propagation by allowing mature virions to exit the infected myocyte and infect adjacent myocytes (24). Moreover, the carboxyl-terminal fragment of 2A proteinase-mediated dystrophin cleavage by itself can cause marked dystrophic cardiomyopathy through myocardial fibrosis, heightened susceptibility to myocardial ischemic injury, and increased mortality during cardiac stress (28). It should be noted that overall viral protein expression by TD replicons remained lower than that of wild-type RNAs, as demonstrated by the luciferase levels at 4 h posttransfection in cardiomyocytes (Fig. 2). This decreased expression would still be sufficient to cause the onset of DCM, as demonstrated in a murine model expressing 2A via cellular transcripts driven by the alpha-myosin heavy chain (α-MHC) promoter, which would be more akin to a chronic pattern of 2A expression in persistently infected cardiomyocytes than to a fulminant CVB3 infection (23). Nevertheless, additional studies will be required to determine if dystrophin is cleaved in cardiomyocytes persistently infected with TD viruses.

Although replicons corresponding to TD viral genomes can synthesize viral proteins, their RNA synthesis levels are greatly reduced. Our in vitro replication experiments did not show detectable levels of RNA synthesis for deletions larger than 21 nucleotides. Moreover, the RNA detected was double stranded without isolated single-stranded, positive-sense RNA. These in vitro results were confirmed by our data from transfection of deleted luciferase replicons into cardiomyocytes showing a lack of luciferase signal amplification from 4 h posttransfection, as well as no effect of GuHCl on luciferase signals. Our data strongly suggest an RNA replication defect for the TD viral RNAs. During infection, this defect would likely lead to a positive-strand/negative-strand RNA ratio closer to 1 than to the asymmetric ratio of 30 to 70 that is normally observed during acute infections with wild-type enterovirus strains (37, 38).

Our results confirmed those of a previous study in which no replication was detected following transfection of a CVB3 genome with a 32-nucleotide deletion of the 5' NCR into HeLa cells (49). Other studies have detected very low levels of replication of TD RNAs in HeLa S10 cell in vitro RNA synthesis reactions or with semi-nested reverse transcription (RT)-PCR amplification, even for the deletion of 49 nucleotides (32, 34, 48). The most likely explanation for these differences is that the methods used in our study were not sufficiently sensitive to detect the very low levels of RNA replication directed by the TD30 and TD49 RNAs in vitro. However, Bouin and colleagues recently demonstrated the coexistence of a large majority of TD viral genomes with a minority of wild-type CVB3 genomic RNAs (less than 0.9% of the viruses sequenced) in cardiac biopsy specimens from a patient suffering from DCM. This discovery was facilitated by the use of next-generation sequencing, which enabled the detection of very minor variants representing less than 1% of the total viral RNA population that could not be detected by the Sanger sequencing method used in previous studies (29, 31, 32). It is possible that the replication of this remaining wild-type population of viruses could generate, by a presently unknown mechanism, a majority of viruses with terminally deleted genomic RNAs in cardiomyocytes that are unable to replicate by themselves and a minority of wild-type viruses capable of maintaining a low-level chronic infection. The wild-type virus could also play the role of helper virus, allowing TD viruses to replicate by providing, in trans or through genomic recombination events, the elements necessary for their replication (50–52). Wild-type and TD viruses could reproduce in vivo by using a mode of viral persistence known to occur in cell culture via defective interfering (DI) particles (53). In this model, picornavirus DI populations harboring deletions within the capsid protein-coding region must coexist with the wild-type population, since DI genomes are packaged using capsid proteins produced by wild-type viruses (54–56).

The synthesis of even low levels of double-stranded RNA by TD viruses could be sufficient to induce type I interferon (IFN) secretion by infected cardiomyocytes. Indeed,

dsRNA, known as the replicative form or replicative intermediate, is recognized by cellular sensors, including Toll-like receptors 3 and 7 and RNA helicases, in particular MDA5, causing the virus-infected cardiomyocytes to produce type 1 IFNs and to promote the inflammatory response (57–62). As summarized by Althof and colleagues (63), the local synthesis of type 1 IFNs can be harmful to the myocardium by causing inflammatory-cell infiltration, including CD8$^+$ T cells, macrophages, natural killer cells, and neutrophils, and inflammatory cytokine secretion, thereby causing immune-pathological damages (63–65). The prolonged presence of dsRNA in cardiomyocytes may be associated with long-term morbidity caused by chronic inflammation. Such inflammation could promote immune-mediated tissue damage known to be involved in the pathogenesis of enterovirus-related cardiomyopathy. It remains to be seen if innate immune sensors in cardiomyocytes can detect the very low levels of dsRNA synthesized by terminally deleted viruses and subsequently stimulate type I interferon secretion. Persistent CVB strains must find a way to overcome this antiviral host response, since type I IFNs are efficient effectors of the innate immune response constraining CVB spread, leading to clearance of the virus from the myocardium following acute infection. Type I interferon secretion leads to the transcription of hundreds of interferon-stimulated genes, which display antiviral properties by targeting almost any step of the virus replication cycle (66). Interestingly, Hyde and colleagues demonstrated that alphaviruses, which are also single-stranded, positive-strand RNA viruses, use mutations within the 5′ noncoding region affecting secondary-structural elements of their RNAs to alter interferon-stimulated protein binding and functions (67). Their results suggest an evasion mechanism by which a deleted virus with modified 5′ RNA secondary structures could avoid immune restriction, despite type 1 IFN secretion and interferon-stimulated gene transcription, leading to long-term virus persistence in the heart.

To understand the possible cause(s) of impaired single-stranded RNA synthesis by TD strains of CVB3, we investigated binding to the 5′ ends of deleted positive-strand viral RNAs of cellular (i.e., PCBP2) and viral (i.e., 3CD) factors involved in viral RNA replication. These proteins form a ribonucleoprotein complex with stem-loop I RNA that enables 5′-3′ intramolecular interactions resulting in a protein-protein bridge, template recognition by the polymerase 3D, and RNA replication initiation (68). PCBP2 is primarily a nuclear-resident protein with RNA binding activity that binds stem-loop b of S-L I at the 5′ end of genomic RNA. This interaction displays increased affinity when the precursor to the virally encoded RNA-dependent RNA polymerase 3D^{pol} and the proteinase 3C^{pro}, 3CD^{pro}, is also present on stem-loop d of S-L I, forming a ternary complex that promotes both negative-strand and positive-strand RNA synthesis (7, 10, 40, 69). Loss of the binding sites or modification of RNA secondary structure rendering interaction with these proteins less stable could explain, in part, the severe deficiency in positive-strand RNA synthesis of TD viruses. Indeed, we found that deletions of either 30 or 49 nucleotides of the CVB3 5′ NCR had reduced levels of binding by PCBP2 and 3CD^{pro}, corresponding to RNA synthesis defects exhibited in our *in vitro* RNA replication assays. In particular, 3CD^{pro} binding efficiency was reduced in accordance with the deletion size, since the ribonucleoprotein complex required an increased protein concentration to form. This result suggested that even if primary protein binding sites are conserved despite genomic deletions, RNP complex formation with specific host or viral proteins could be less stable and lead to lower levels of RNA synthesis during infection.

It is known that the host protein hnRNP C can bind both the 3′ and 5′ termini of poliovirus negative-strand RNA intermediates, an interaction proposed to promote the synthesis of positive-strand enterovirus RNA molecules (12, 70, 71). Thus, the 5′-terminal deletions of positive-strand RNAs would lead to deletions in the 3′ ends of negative-strand RNAs, possibly reducing the binding of hnRNP C to these replication intermediates. Loss of such binding might also contribute to the reduction of positive-strand RNA synthesis observed with TD viruses. Moreover, low levels of hnRNP C expression in the cytoplasm of quiescent and differentiated cells (like cardiomyocytes)

have been suggested to give putative hnRNP C-independent TD genomes an evolutionary advantage over hnRNP C-dependent wild-type enterovirus RNA, thereby enabling them to become the dominant virus population in persistent infections (31, 72). Our future studies of RNP complexes formed with the 3′ ends of negative-strand CVB3 RNAs will address the possible roles of hnRNP C, as well as other host and viral proteins, in TD viral replication and their possible link to persistent infections. Overall, to better understand the mechanisms by which genomic deletions impact the synthesis efficiency of negative- and positive-strand viral RNAs, a complete identification of the replication complexes used by wild-type and terminally deleted CVB3 RNAs in cardiomyocytes will be required. This identification could help in designing new therapeutic strategies either targeting viral proteins or inhibiting host protein activities involved in viral RNA replication to treat persistent enterovirus cardiac infections mediated by TD strains.

MATERIALS AND METHODS

Coxsackievirus cDNA clones. Six previously described cDNA clones of coxsackievirus B3 strains were used in this study. Two of the cDNAs contain full-length wild-type CVB3 RNA genomes. pCVB3-28 contains the cDNA genome of the cardiovirulent CVB3 strain 28 (GenBank accession no. AY752944.2) with a ribozyme designed to cleave T7 RNA polymerase transcripts at nucleotide 1 of the genome (73, 74). pCVB3-0 contains the cDNA of the noncardiovirulent CVB3 strain 0 (GenBank accession no. AY752945.1), initially described by Charles Gauntt and differing in only 1 nucleotide at position 234 (U in CVB3/28; C in CVB/0) from CVB3 strain 28 (74–76). Four of the cDNAs contain terminally deleted CVB3 genomes. pCVB3-TD7, pCVB3-TD30, and pCVB3-TD49 are variants of pCVB3-28 in which 5′-terminal deletions of 7, 30, and 49 nucleotides, respectively, were engineered into the pCVB3-28 genome with a ribozyme to ensure cleavage at the authentic 5′-terminal nucleotide of each genome (32). pCVB3-TD21 contains the 5′-terminal sequence of a virus detected in the heart in a fatal human case of CVB2 infection engineered into pCVB3-28 as described above but with a ribozyme designed to ensure cleavage at the 22nd nucleotide to generate a deletion of 21 nucleotides relative to wild-type RNA (30).

Cardiomyocytes. Two types of cardiac cell lines were used in this study. Primary HCM (ScienCell Research Laboratories) isolated from human heart were maintained in cardiac myocyte medium (ScienCell Research Laboratories) in tissue culture flasks coated with poly-L-lysine. Primary cell cultures were used between passages 4 and 15. HL-1 cells are a cardiac myocyte line that can be repeatedly passaged and yet maintain a cardiac-specific phenotype. The HL-1 cell line was established from an AT-1 subcutaneous tumor excised from an adult female Jackson Laboratory C57BL/6J mouse. The cells were maintained in Claycomb medium (Sigma) and plated in tissue culture flasks coated overnight with gelatin (0.02% [wt/vol]) and fibronectin (0.5% [vol/vol]) (77).

RNA transcript preparation. Plasmids corresponding to full-length wild-type and terminally deleted forms of CVB RNAs were linearized with the restriction enzyme ClaI. Transcription reactions were performed with T7 RNA polymerase using a Megascript T7 transcription kit (Ambion). Fifty-microliter transcription reaction mixtures were incubated for 4 h at 37°C and terminated by treatment with DNase I for 15 min at 37°C. RNAs were purified using an RNeasy minikit (Qiagen). For *in vitro* translation-replication reactions, RNAs were additionally purified by phenol-chloroform extractions and precipitated with ethanol.

In vitro translation and RNA replication reactions. The coupled *in vitro* translation and RNA replication assays were carried out as described previously (78). Briefly, translation-replication mixtures (50 μl total) contained 60% (vol/vol) macrococcal nuclease-treated HeLa S10 cytoplasmic extract, 3 μg *in vitro*-transcribed CVB3 RNA, and all-4 buffer containing reduced levels of CTP (1 mM ATP, 0.25 mM GTP, 0.25 mM UTP, 0.01 mM CTP [GE Healthcare Life Sciences], 60 mM potassium acetate, 30 mM creatine phosphate, 0.4 mg/ml creatine kinase, 20 mM HEPES-KOH [pH 7.4]). The reaction mixtures were then split into two portions, with 10 μl for translation and the remaining 40 μl for RNA replication. Ten μCi [^{35}S]methionine (PerkinElmer) was added to the translation reaction mixture, which was incubated for 6 h at 30°C, supplemented with 2× Laemmli sample buffer (LSB), and boiled. The translation products were resolved by SDS-PAGE (12.5% resolving gel; 5% stacking gel), followed by fluorography. The RNA replication mixture was incubated at 30°C for 4.5 h before 25 μCi [^{32}P]CTP (PerkinElmer) was added, and the reaction mixture was incubated for an additional 2 h at 34°C. The RNA replication product was then purified using an RNeasy minikit (Qiagen) and separated on a 1.1% agarose gel. The levels of 18S and 28S rRNA in each lane, as determined by examination of ethidium bromide-stained gels under UV light, were used to confirm equal loading of samples in the gel. Both translation and RNA replication gels were subjected to autoradiography on phosphor screens, performed using a Personal Molecular Imager FX (Bio-Rad) and analyzed with Quantity One software (Bio-Rad).

Luciferase replicons, transfection of cardiomyocytes, and luciferase assays. The CVB3 replicon (pRib-CVB3-RLuc; kindly provided by Martijn Langereis and Frank van Kuppeveld) contains a CVB3 cDNA in which the P1 capsid coding region has been replaced by the *Renilla* luciferase gene. The cDNA was cloned downstream from a hammerhead ribozyme sequence to remove nonviral nucleotides from the 5′ ends of transcript RNAs (79). To generate 5′-terminally deleted CVB3 *Renilla* luciferase replicons harboring genomic deletions with sizes identical to those tested using *in vitro* translation and RNA replication assays, the pRib-CVB3-RLuc replicon, as well as CVB3 cDNA clones (pCVB3-28, pCVB3-TD7,

pCVB3-TD21, pCVB3-TD30, and pCVB3-TD49), were doubly digested with BlpI and XmaI restriction enzymes. A fragment of 330 nucleotides encompassing the ribozyme and the 5′ end of the viral genome was removed from the wild-type (pCVB3-28) and the four 5′-terminally deleted (pCVB3-TD7, pCVB3-TD21, pCVB3-TD30, and pCVB3-TD49) CVB3 cDNA constructs and gel purified. In addition, the digested pRib-CVB3-RLuc replicon vector was isolated and gel purified. The 330-nucleotide fragments removed from CVB3 cDNA constructs were cloned into the pRib-CVB3-RLuc replicon vector. The CVB3-0 replicon was generated from the CVB3-28 replicon by site-directed mutagenesis of nucleotide position 234 (T in CVB3/28; C in CVB/0).

For RNA transfection experiments, ∼90% confluent monolayers of cardiac myocytes (HCM or HL-1 cells) grown in six-well plates were rinsed twice with phosphate-buffered saline (PBS). A transfection mixture consisting of 2 μg of replicon RNA, 250 μl of optiMEM (ThermoFisher Scientific), 5 μl of mRNA Boost reagent, and 5 μl of a TransIT mRNA transfection kit (Mirus) was incubated for 5 min at room temperature and then added to each well. Cultures were incubated at 37°C for 2, 4, 6, or 8 h. Parallel transfections and subsequent incubations were carried out in the presence of 2 mM guanidine hydrochloride to prevent RNA replication and to allow the measurement of luciferase levels at each time point that resulted solely from the translation of input replicon RNA. At the indicated times posttransfection, cells were washed twice with PBS. A *Renilla* luciferase assay (Promega) was used for quantitation of luciferase activity. Cell monolayers were harvested with 500 μl of lysis buffer added to each well, and cell lysates were collected in 1.5-ml Eppendorf tubes. A volume of 20 μl of lysate was used in luciferase assays with the addition of 100 μl of luciferin substrate, and light emission was measured with a Monolight 2010 luminometer (Analytical Luminescence Laboratory). Triplicate samples were analyzed for each time point, and each time course experiment was performed three times.

Electrophoretic mobility shift assays. RNA mobility shift assays were performed as previously described (78, 80). Briefly, increasing amounts of purified recombinant PCBP2 (molar concentrations ranged from 2.5 to 7.5 μM) and/or recombinant purified 3CD^{pro} [3CD(μ10)] (molar concentrations ranged from 0.05 to 10 μM) were incubated in the presence of RNA binding buffer (5 mM HEPES-KOH [pH 7.4], 25 mM KCl, 2.5 mM MgCl$_2$, 20 mM dithiothreitol, 3.8% [vol/vol] glycerol, 1 mg/ml of *Escherichia coli* tRNA [Sigma], 8 U of RNasin [Promega] RNase inhibitor, and 0.5 mg/ml of bovine serum albumin [New England BioLabs]) with [^{32}P]UTP (PerkinElmer)-radiolabeled wild-type or 5′-terminally deleted RNA probe derived from transcription of CVB3 cDNA clones linearized with XmnI restriction enzyme. The final concentration of probe was 0.1 nM contained within a total reaction volume of 10 μl. This reaction mixture was incubated for 10 min at 30°C. Following incubation, 2.5 μl of 50% glycerol was added, and the resulting complexes were resolved at 4°C on native 4% polyacrylamide gels containing 5% glycerol in Tris-borate-EDTA (TBE) buffer. Images were generated from scans of phosphor screens performed using a Personal Molecular Imager FX (Bio-Rad) and analyzed using Quantity One software.

ACKNOWLEDGMENTS

REFERENCES

1. Racaniello VR. 2013. Picornaviridae: the viruses and their replication, p 453–489. *In* Knipe DM, Howley PM (ed), Fields virology. Lippincott Williams & Wilkins, Philadelphia, PA.
2. Brown DM, Kauder SE, Cornell CT, Jang GM, Racaniello VR, Semler BL. 2004. Cell-dependent role for the poliovirus 3′ noncoding region in positive-strand RNA synthesis. J Virol 78:1344–1351. https://doi.org/10.1128/JVI.78.3.1344-1351.2004.
3. Sean P, Semler BL. 2008. Coxsackievirus B RNA replication: lessons from poliovirus. Curr Top Microbiol Immunol 323:89–121.
4. Toyoda H, Franco D, Fujita K, Paul AV, Wimmer E. 2007. Replication of poliovirus requires binding of the poly(rC) binding protein to the cloverleaf as well as to the adjacent C-rich spacer sequence between the cloverleaf and the internal ribosomal entry site. J Virol 81:10017–10028. https://doi.org/10.1128/JVI.00516-07.
5. Andino R, Rieckhof GE, Achacoso PL, Baltimore D. 1993. Poliovirus RNA synthesis utilizes an RNP complex formed around the 5′-end of viral RNA. EMBO J 12:3587–3598.
6. Andino R, Rieckhof GE, Baltimore D. 1990. A functional ribonucleoprotein complex forms around the 5′ end of poliovirus RNA. Cell 63:369–380. https://doi.org/10.1016/0092-8674(90)90170-J.
7. Parsley TB, Towner JS, Blyn LB, Ehrenfeld E, Semler BL. 1997. Poly(rC) binding protein 2 forms a ternary complex with the 5′-terminal sequences of poliovirus RNA and the viral 3CD proteinase. RNA 3:1124–1134.
8. Ohlenschläger O, Wöhnert J, Bucci E, Seitz S, Häfner S, Ramachandran R, Zell R, Görlach M. 2004. The structure of the stemloop D subdomain of coxsackievirus B3 cloverleaf RNA and its interaction with the proteinase 3C. Structure 12:237–248.

9. Zell R, Sidigi K, Bucci E, Stelzner A, Görlach M. 2002. Determinants of the recognition of enteroviral cloverleaf RNA by coxsackievirus B3 proteinase 3C. RNA 8:188–201. https://doi.org/10.1017/S1355838202012785.

10. Vogt DA, Andino R. 2010. An RNA element at the 5′-end of the poliovirus genome functions as a general promoter for RNA synthesis. PLoS Pathog 6:e1000936. https://doi.org/10.1371/journal.ppat.1000936.

11. Zell R, Ihle Y, Seitz S, Gundel U, Wutzler P, Gorlach M. 2008. Poly(rC)-binding protein 2 interacts with the oligo(rC) tract of coxsackievirus B3. Biochem Biophys Res Commun 366:917–921. https://doi.org/10.1016/j.bbrc.2007.12.038.

12. Brunner JE, Nguyen JHC, Roehl HH, Ho TV, Swiderek KM, Semler BL. 2005. Functional interaction of heterogeneous nuclear ribonucleoprotein C with poliovirus RNA synthesis initiation complexes. J Virol 79:3254–3266. https://doi.org/10.1128/JVI.79.6.3254-3266.2005.

13. Herold J, Andino R. 2000. Poliovirus requires a precise 5′ end for efficient positive-strand RNA synthesis. J Virol 74:6394–6400. https://doi.org/10.1128/JVI.74.14.6394-6400.2000.

14. Cooper LT, Baughman KL, Feldman AM, Frustaci A, Jessup M, Kuhl U, Levine GN, Narula J, Starling RC, Towbin J, Virmani R, American Heart Association, American College of Cardiology, European Society of Cardiology, Heart Failure Society of America, Heart Failure Association of the European Society of Cardiology. 2007. The role of endomyocardial biopsy in the management of cardiovascular disease. J Am Coll Cardiol 50:1914–1931. https://doi.org/10.1016/j.jacc.2007.09.008.

15. Dennert R, Crijns HJ, Heymans S. 2008. Acute viral myocarditis. Eur Heart J 29:2073–2082. https://doi.org/10.1093/eurheartj/ehn296.

16. Rey L, Lambert V, Wattré P, Andréoletti L. 2001. Detection of enteroviruses ribonucleic acid sequences in endomyocardial tissue from adult patients with chronic dilated cardiomyopathy by a rapid RT-PCR and hybridization assay. J Med Virol 64:133–140. https://doi.org/10.1002/jmv.1028.

17. Andréoletti L, Bourlet T, Moukassa D, Rey L, Hot D, Li Y, Lambert V, Gosselin B, Mosnier JF, Stankowiak C, Wattré P. 2000. Enteroviruses can persist with or without active viral replication in cardiac tissue of patients with end-stage ischemic or dilated cardiomyopathy. J Infect Dis 182:1222–1227. https://doi.org/10.1086/315818.

18. Li Y, Bourlet T, Andreoletti L, Mosnier JF, Peng T, Yang Y, Archard LC, Pozzetto B, Zhang H. 2000. Enteroviral capsid protein VP1 is present in myocardial tissues from some patients with myocarditis or dilated cardiomyopathy. Circulation 101:231–234. https://doi.org/10.1161/01.CIR.101.3.231.

19. Andreoletti L, Hober D, Decoene C, Copin MC, Lobert PE, Dewilde A, Stankowiac C, Wattre P. 1996. Detection of enteroviral RNA by polymerase chain reaction in endomyocardial tissue of patients with chronic cardiac diseases. J Med Virol 48:53–59. https://doi.org/10.1002/(SICI)1096-9071(199601)48:1<53::AID-JMV9>3.0.CO;2-K.

20. Andreoletti L, Wattre P, Decoene C, Lobert PE, Dewilde A, Hober D. 1995. Detection of enterovirus-specific RNA sequences in explanted myocardium biopsy specimens from patients with dilated or ischemic cardiomyopathy. Clin Infect Dis 21:1315–1317. https://doi.org/10.1093/clinids/21.5.1315.

21. Kim KS, Hufnagel G, Chapman NM, Tracy S. 2001. The group B coxsackieviruses and myocarditis. Rev Med Virol 11:355–368. https://doi.org/10.1002/rmv.326.

22. Rakar S, Sinagra G, Di Lenarda A, Poletti A, Bussani R, Silvestri F, Camerini F. 1997. Epidemiology of dilated cardiomyopathy. A prospective postmortem study of 5252 necropsies. The Heart Muscle Disease Study Group. Eur Heart J 18:117–123.

23. Xiong D, Yajima T, Lim B-K, Stenbit A, Dublin A, Dalton ND, Summers-Torres D, Molkentin JD, Duplain H, Wessely R, Chen J, Knowlton KU. 2007. Inducible cardiac-restricted expression of enteroviral protease 2A is sufficient to induce dilated cardiomyopathy. Circulation 115:94–102.

24. Lim B-K, Peter AK, Xiong D, Narezkina A, Yung A, Dalton ND, Hwang K-K, Yajima T, Chen J, Knowlton KU. 2013. Inhibition of coxsackievirus-associated dystrophin cleavage prevents cardiomyopathy. J Clin Invest 123:5146–5151. https://doi.org/10.1172/JCl66271.

25. Andréoletti L, Ventéo L, Douche-Aourik F, Canas F, Lorin de la Grand-maison G, Jacques J, Moret H, Jovenin N, Mosnier J-F, Matta M, Duband S, Pluot M, Pozzetto B, Bourlet T. 2007. Active coxsackieviral B infection is associated with disruption of dystrophin in endomyocardial tissue of patients who died suddenly of acute myocardial infarction. J Am Coll Cardiol 50:2207–2214. https://doi.org/10.1016/j.jacc.2007.07.080.

26. Badorff C, Berkely N, Mehrotra S, Talhouk JW, Rhoads RE, Knowlton KU. 2000. Enteroviral protease 2A directly cleaves dystrophin and is inhibited by a dystrophin-based substrate analogue. J Biol Chem 275:11191–11197. https://doi.org/10.1074/jbc.275.15.11191.

27. Badorff C, Lee GH, Lamphear BJ, Martone ME, Campbell KP, Rhoads RE, Knowlton KU. 1999. Enteroviral protease 2A cleaves dystrophin: evidence of cytoskeletal disruption in an acquired cardiomyopathy. Nat Med 5:320–326. https://doi.org/10.1038/6543.

28. Barnabei MS, Sjaastad FV, Townsend D, Bedada FB, Metzger JM. 2015. Severe dystrophic cardiomyopathy caused by the enteroviral protease 2A-mediated C-terminal dystrophin cleavage fragment. Sci Transl Med 7:294ra106. https://doi.org/10.1126/scitranslmed.aaa4804.

29. Bouin A, Nguyen Y, Wehbe M, Renois F, Fornes P, Bani-Sadr F, Metz D, Andreoletti L. 2016. Major persistent 5′ terminally deleted coxsackievirus B3 populations in human endomyocardial tissues. Emerg Infect Dis 22:1488–1490. https://doi.org/10.3201/eid2208.160186.

30. Chapman NM, Kim K-S, Drescher KM, Oka K, Tracy S. 2008. 5′ terminal deletions in the genome of a coxsackievirus B2 strain occurred naturally in human heart. Virology 375:480–491. https://doi.org/10.1016/j.virol.2008.02.030.

31. Kim KS, Chapman NM, Tracy S. 2008. Replication of coxsackievirus B3 in primary cell cultures generates novel viral genome deletions. J Virol 82:2033–2037. https://doi.org/10.1128/JVI.01774-07.

32. Kim KS, Tracy S, Tapprich W, Bailey J, Lee CK, Kim K, Barry WH, Chapman NM. 2005. 5′-terminal deletions occur in coxsackievirus B3 during replication in murine hearts and cardiac myocyte cultures and correlate with encapsidation of negative-strand viral RNA. J Virol 79:7024–7041. https://doi.org/10.1128/JVI.79.11.7024-7041.2005.

33. Liu Y, Wimmer E, Paul AV. 2009. Cis-acting RNA elements in human and animal plus-strand RNA viruses. Biochim Biophys Acta 1789:495–517. https://doi.org/10.1016/j.bbagrm.2009.09.007.

34. Sharma N, Ogram SA, Morasco BJ, Spear A, Chapman NM, Flanegan JB. 2009. Functional role of the 5′ terminal cloverleaf in coxsackievirus RNA replication. Virology 393:238–249. https://doi.org/10.1016/j.virol.2009.07.039.

35. Barton DJ, O'Donnell BJ, Flanegan JB. 2001. 5′ cloverleaf in poliovirus RNA is a cis-acting replication element required for negative-strand synthesis. EMBO J 20:1439–1448. https://doi.org/10.1093/emboj/20.6.1439.

36. Lévêque N, Renois F, Talmud D, Nguyen Y, Lesaffre F, Boulagnon C, Bruneval P, Fornes P, Andréoletti L. 2012. Quantitative genomic and antigenomic enterovirus RNA detection in explanted heart tissue samples from patients with end-stage idiopathic dilated cardiomyopathy. J Clin Microbiol 50:3378–3380. https://doi.org/10.1128/JCM.01612-12.

37. Giachetti C, Semler BL. 1991. Role of a viral membrane polypeptide in strand-specific initiation of poliovirus RNA synthesis. J Virol 65:2647–2654.

38. Novak JE, Kirkegaard K. 1991. Improved method for detecting poliovirus negative strands used to demonstrate specificity of positive-strand encapsidation and the ratio of positive to negative strands in infected cells. J Virol 65:3384–3387.

39. Pincus SE, Diamond DC, Emini EA, Wimmer E. 1986. Guanidine-selected mutants of poliovirus: mapping of point mutations to polypeptide 2C. J Virol 57:638–646.

40. Gamarnik AV, Andino R. 2000. Interactions of viral protein 3CD and poly(rC) binding protein with the 5′ untranslated region of the poliovirus genome. J Virol 74:2219–2226. https://doi.org/10.1128/JVI.74.5.2219-2226.2000.

41. Pallansch MA, Oberste MS, Whitton JL. 2013. Enteroviruses: polioviruses, coxsackieviruses, echoviruses, and newer enteroviruses, p 490–530. In Knipe DM, Howley PM (ed), Fields virology. Lippincott Williams & Wilkins, Philadelphia, PA.

42. Tracy S, Drescher KM, Chapman NM. 2011. Enteroviruses and type 1 diabetes. Diabetes Metab Res Rev 27:820–823. https://doi.org/10.1002/dmrr.1255.

43. Chapman NM, Kim KS. 2008. Persistent coxsackievirus infection: enterovirus persistence in chronic myocarditis and dilated cardiomyopathy. Curr Top Microbiol Immunol 323:275–292.

44. Douche-Aourik F, Berlier W, Féasson L, Bourlet T, Harrath R, Omar S, Grattard F, Denis C, Pozzetto B. 2003. Detection of enterovirus in human skeletal muscle from patients with chronic inflammatory muscle disease or fibromyalgia and healthy subjects. J Med Virol 71:540–547. https://doi.org/10.1002/jmv.10531.

45. Vandenberghe N, Leveque N, Corcia P, Brunaud-Danel V, Salort-Campana E, Besson G, Tranchant C, Clavelou P, Beaulieux F, Ecochard R, Vial C, Brous-solle E, Lina B. 2010. Cerebrospinal fluid detection of enterovirus genome in

ALS: a study of 242 patients and 354 controls. Amyotroph Lateral Scler 11:277–282. https://doi.org/10.3109/17482960903262083.

46. Muir P, Nicholson F, Sharief MK, Thompson EJ, Cairns NJ, Lantos P, Spencer GT, Kaminski HJ, Banatvala JE. 1995. Evidence for persistent enterovirus infection of the central nervous system in patients with previous paralytic poliomyelitis. Ann N Y Acad Sci 753:219–232. https://doi.org/10.1111/j.1749-6632.1995.tb27548.x.

47. Cunningham L, Bowles NE, Lane RJ, Dubowitz V, Archard LC. 1990. Persistence of enteroviral RNA in chronic fatigue syndrome is associated with the abnormal production of equal amounts of positive and negative strands of enteroviral RNA. J Gen Virol 71:1399–1402. https://doi.org/10.1099/0022-1317-71-6-1399.

48. Smithee S, Tracy S, Chapman NM. 2015. Mutational disruption of cis-acting replication element 2C in coxsackievirus B3 leads to 5′-terminal genomic deletions. J Virol 89:11761–11772. https://doi.org/10.1128/JVI.01308-15.

49. Hunziker IP, Cornell CT, Whitton JL. 2007. Deletions within the 5′UTR of coxsackievirus B3: consequences for virus translation and replication. Virology 360:120–128. https://doi.org/10.1016/j.virol.2006.09.041.

50. Muslin C, Joffret M, Pelletier I, Blondel B, Delpeyroux F. 2015. Evolution and emergence of enteroviruses through intra- and inter-species recombination: plasticity and phenotypic impact of modular genetic exchanges in the 5′ untranslated region. PLoS Pathog 11:e1005266. https://doi.org/10.1371/journal.ppat.1005266.

51. Holmblat B, Jégouic S, Muslin C, Blondel B, Joffret M-L, Delpeyroux F. 2014. Nonhomologous recombination between defective poliovirus and coxsackievirus genomes suggests a new model of genetic plasticity for picornaviruses. mBio 5:e01119–01114. https://doi.org/10.1128/mBio.01119-14.

52. Collis PS, BJ O'Donnell Barton DJ, Rogers JA, Flanegan JB. 1992. Replication of poliovirus RNA and subgenomic RNA transcripts in transfected cells. J Virol 66:6480–6488.

53. Holland JJ, Villarreal LP. 1974. Persistent noncytocidal vesicular stomatitis virus infections mediated by defective T particles that suppress virion transcriptase. Proc Natl Acad Sci U S A 71:2956–2960. https://doi.org/10.1073/pnas.71.8.2956.

54. McClure MA, Holland JJ, Perrault J. 1980. Generation of defective interfering particles in picornaviruses. Virology 100:408–418. https://doi.org/10.1016/0042-6822(80)90532-2.

55. Cole CN, Smoler D, Wimmer E, Baltimore D. 1971. Defective interfering particles of poliovirus. I. Isolation and physical properties. J Virol 7:478–485.

56. McLaren LC, Holland JJ. 1974. Defective interfering particles from poliovirus vaccine and vaccine reference strains. Virology 60:579–583. https://doi.org/10.1016/0042-6822(74)90352-3.

57. Mukherjee A, Morosky SA, Delorme-Axford E, Dybdahl-Sissoko N, Oberste MS, Wang T, Coyne CB. 2011. The coxsackievirus B 3C protease cleaves MAVS and TRIF to attenuate host type I interferon and apoptotic signaling. PLoS Pathog 7:e1001311. https://doi.org/10.1371/journal.ppat.1001311.

58. Wang JP, Cerny A, Asher DR, Kurt-Jones EA, Bronson RT, Finberg RW. 2010. MDA5 and MAVS mediate type I interferon responses to coxsackie B virus. J Virol 84:254–260. https://doi.org/10.1128/JVI.00631-09.

59. Hardarson HS, Baker JS, Yang Z, Purevjav E, Huang C-H, Alexopoulou L, Li N, Flavell RA, Bowles NE, Vallejo JG. 2007. Toll-like receptor 3 is an essential component of the innate stress response in virus-induced cardiac injury. Am J Physiol Heart Circ Physiol 292:H251–H258. https://doi.org/10.1152/ajpheart.00398.2006.

60. Wang JP, Asher DR, Chan M, Kurt-Jones EA, Finberg RW. 2007. Cutting edge: antibody-mediated TLR7-dependent recognition of viral RNA. J Immunol 178:3363–3367. https://doi.org/10.4049/jimmunol.178.6.3363.

61. Fuse K, Chan G, Liu Y, Gudgeon P, Husain M, Chen M, Yeh W-C, Akira S, Liu PP. 2005. Myeloid differentiation factor-88 plays a crucial role in the pathogenesis of coxsackievirus B3-induced myocarditis and influences type I interferon production. Circulation 112:2276–2285. https://doi.org/10.1161/CIRCULATIONAHA.105.536433.

62. Feng Q, Hato SV, Langereis MA, Zoll J, Virgen-Slane R, Peisley A, Hur S, Semler BL, van Rij RP, van Kuppeveld FJ. 2012. MDA5 detects the double-stranded RNA replicative form in picornavirus-infected cells. Cell Rep 2:1187–1196. https://doi.org/10.1016/j.celrep.2012.10.005.

63. Althof N, Harkins S, Kemball CC, Flynn CT, Alirezaei M, Whitton JL. 2014.

In vivo ablation of type I interferon receptor from cardiomyocytes delays coxsackieviral clearance and accelerates myocardial disease. J Virol 88:5087–5099. https://doi.org/10.1128/JVI.00184-14.

64. Henke A, Huber S, Stelzner A, Whitton JL. 1995. The role of CD8+ T lymphocytes in coxsackievirus B3-induced myocarditis. J Virol 69:6720–6728.

65. Chow LH, Beisel KW, McManus BM. 1992. Enteroviral infection of mice with severe combined immunodeficiency. Evidence for direct viral pathogenesis of myocardial injury. Lab Invest 66:24–31.

66. Schoggins JW, Rice CM. 2011. Interferon-stimulated genes and their antiviral effector functions. Curr Opin Virol 1:519–525. https://doi.org/10.1016/j.coviro.2011.10.008.

67. Hyde JL, Gardner CL, Kimura T, White JP, Liu G, Trobaugh DW, Huang C, Tonelli M, Paessler S, Takeda K, Klimstra WB, Amarasinghe GK, Diamond MS. 2014. A viral RNA structural element alters host recognition of nonself RNA. Science 343:783–787. https://doi.org/10.1126/science.1248465.

68. Tuschall DM, Hiebert E, Flanegan JB. 1982. Poliovirus RNA-dependent RNA polymerase synthesizes full-length copies of poliovirion RNA, cellular mRNA, and several plant virus RNAs in vitro. J Virol 44:209–216.

69. Gamarnik AV, Andino R. 1998. Switch from translation to RNA replication in a positive-stranded RNA virus. Genes Dev 12:2293–2304. https://doi.org/10.1101/gad.12.15.2293.

70. Ertel KJ, Brunner JE, Semler BL. 2010. Mechanistic consequences of hnRNP C binding to both RNA termini of poliovirus negative-strand RNA intermediates. J Virol 84:4229–4242. https://doi.org/10.1128/JVI.02198-09.

71. Roehl HH, Semler BL. 1995. Poliovirus infection enhances the formation of two ribonucleoprotein complexes at the 3′ end of viral negative-strand RNA. J Virol 69:2954–2961.

72. Brunner JE, Ertel KJ, Rozovics JM, Semler BL. 2010. Delayed kinetics of poliovirus RNA synthesis in a human cell line with reduced levels of hnRNP C proteins. Virology 400:240–247. https://doi.org/10.1016/j.virol.2010.01.031.

73. Tracy S, Drescher KM, Chapman NM, Kim KS, Carson SD, Pirruccello S, Lane PH, Romero JR, Leser JS. 2002. Toward testing the hypothesis that group B coxsackieviruses (CVB) trigger insulin-dependent diabetes: inoculating nonobese diabetic mice with CVB markedly lowers diabetes incidence. J Virol 76:12097–12111. https://doi.org/10.1128/JVI.76.23.12097-12111.2002.

74. Tu Z, Chapman NM, Hufnagel G, Tracy S, Romero JR, Barry WH, Zhao L, Currey K, Shapiro B. 1995. The cardiovirulent phenotype of coxsackievirus B3 is determined at a single site in the genomic 5′ nontranslated region. J Virol 69:4607–4618.

75. Chapman NM, Tu Z, Tracy S, Gauntt CJ. 1994. An infectious cDNA copy of the genome of a non-cardiovirulent coxsackievirus B3 strain: its complete sequence analysis and comparison to the genomes of cardiovirulent coxsackieviruses. Arch Virol 135:115–130. https://doi.org/10.1007/BF01309769.

76. Gauntt CJ, Trousdale MD, LaBadie DR, Paque RE, Nealon T. 1979. Properties of coxsackievirus B3 variants which are amyocarditic or myocarditic for mice. J Med Virol 3:207–220. https://doi.org/10.1002/jmv.1890030307.

77. Claycomb WC, Lanson NA, Stallworth BS, Egeland DB, Delcarpio JB, Bahinski A, Izzo NJ. 1998. HL-1 cells: a cardiac muscle cell line that contracts and retains phenotypic characteristics of the adult cardiomyocyte. Proc Natl Acad Sci U S A 95:2979–2984. https://doi.org/10.1073/pnas.95.6.2979.

78. Walter BL, Parsley TB, Ehrenfeld E, Semler BL. 2002. Distinct poly(rC) binding protein KH domain determinants for poliovirus translation initiation and viral RNA replication. J Virol 76:12008–12022. https://doi.org/10.1128/JVI.76.23.12008-12022.2002.

79. Lanke KHW, van der Schaar HM, Belov GA, Feng Q, Duijsings D, Jackson CL, Ehrenfeld E, van Kuppeveld FJM. 2009. GBF1, a guanine nucleotide exchange factor for Arf, is crucial for coxsackievirus B3 RNA replication. J Virol 83:11940–11949. https://doi.org/10.1128/JVI.01244-09.

80. Blair WS, Nguyen JH, Parsley TB, Semler BL. 1996. Mutations in the poliovirus 3CD proteinase S1-specificity pocket affect substrate recognition and RNA binding. Virology 218:1–13. https://doi.org/10.1006/viro.1996.0160.